Effects of data acquisition parameters on the quality of sonoelastographic imaging

Gabriela Torres, *Member*, *IEEE*, Juvenal Ormachea, Student *Member*, *IEEE*, Roberto J. Lavarello, *Senior Member*, *IEEE*, Kevin J. Parker, *Fellow*, *IEEE*, and Benjamín Castañeda, *Senior Member*, *IEEE*

Abstract— **Sonoelastography is an ultrasonic technique that provides qualitative and quantitative images of tissue elasticity. Even though the Kasai variance estimator is a key part of the sonoelastographic image formation, there are no studies that demonstrate that its performance using discrete time signals and finite sized ensemble lengths is optimal. In this work, the influence of the selection of acquisition parameters (pulse repetition frequency or PRF, vibration frequency, and ensemble length) on the quality of the elastograms is studied. Simulations are carried out to define the optimal PRF and ensemble length given a vibration frequency in order to avoid artifacts which can severely degrade image quality. This empirical criterion is supported by sonoelastography experiments performed using two commercial scanners, where the variability increased from 4% to 42% at the worst selection of acquisition parameters. Although a further mathematical proof of the empirical findings is required, these results suggest that careful selection of PRF, vibration frequency and ensemble lengths is required to ensure unbiased sonoelastograms.**

I. Introduction

Elastography methods encompass different techniques for tissue characterization using noninvasive assessments of elasticity. Imaging the elastic properties of tissues is an important tool for clinical diagnosis, and its usefulness has been demonstrated for the assessment of liver fibrosis and the characterization of tumors in the breast and prostate, among other applications [1, 2]. Elastography methods, both qualitative and quantitative, have been developed using ultrasound [2], magnetic resonance [3] and optical coherence tomography [4] for observing the tissue displacements induced by either mechanical vibrations or acoustic radiation forces.

In particular, sonoelastography estimates tissue elasticity using pulsed wave Doppler methods such as the Kasai estimator [1]. Qualitative imaging can be performed using a single vibration source and estimating the spectral variance, which is related to the amplitude of the induced tissue vibration [5]. Quantitative imaging can be performed using two vibration sources opposing each other and estimating the spectral shift, which is related to the shear wave speed [5, 6].

*Research supported in part by PUCP PADET 2014 Student Support Program. Research supported in part by N°205-FINCyT-IA-2013

G. Torres, R. Lavarello and B. Castañeda are with the Laboratorio de Imágenes Médicas, Departamento de Ingeniería, Pontificia Universidad Católica del Perú, Lima 32, Peru (e-mail: castaneda.b@pucp.edu.pe).

J. Ormachea and K. J. Parker are with the Electrical and Computer Engineering Department, University of Rochester, Rochester, NY 14620, New York, USA.

Although the Kasai estimator is commonly used in ultrasound systems, there are no studies that demonstrate that its performance using discrete time signals and finite sized ensemble lengths is optimal. Furthermore, recent studies suggest that the performance of the Kasai estimator is dependent on the parameters used for data acquisition. For example, Chan et al. recently reported that the estimator's performance degrades when the acquisition rate increases [8]. Therefore, it is important to understand the effects of the acquisition parameters in the quality of sonoelastography.

The goal of this study is to understand the effects of the choice of pulse repetition frequency (PRF), vibration frequency and ensemble length using the Kasai estimator to construct sonoelastography images. Experiments were developed using two scanners to image homogeneous phantoms.

II. Method

A. Sonoelastography Image Formation

In sonoelastography, sinusoidal vibration is induced in the tissue by external mechanical actuators and a Doppler imaging sequence is used to generate a power spectrum of echoes from the vibrating scatterers. Radiofrequency data is acquired consecutively for a defined number of repetitions (ensemble length) at a given PRF. Sonoelastography data is then constructed by applying Kasai's algorithm to estimate the variance of the slow-time Doppler spectrum,

$$\sigma^2 = \frac{2}{PRP}\left(1 - \frac{|R(PRP)|}{R(0)}\right) \quad [1]$$

where σ^2 is the spectral variance and *R(x)* is the autocorrelation of the phase and quadrature signals obtained for one ensemble after a two-point wall filter is applied. This process is repeated for several lines of data to form an image, where the estimated variance is proportional to the squared amplitude of the vibration in the tissue. Typical sonoelastographic experimental setup and images can be seen in Figures 2B and 7, respectively.

B. Relationship between PRF and Vibration Frequency

PRF can be understood as a sampling rate of the signal provided by the vibration frequency (f_v) from the external source. Since there is a dependence of the Kasai variance estimator on the starting phase of the analyzed signal, the PRF should be selected as a multiple of f_v that maintains the sampling periodicity to minimize the variability of the results. To validate this observation, the following simulation is proposed: for a given sinusoid, the variation coefficient of the Kasai's variance estimator is calculated by simulating PRF sampling values between 6 and 8 times the frequency of vibration. The simulation scheme for a case of a vibration frequency of 100 Hz and ensemble length of 16 is shown in Figure 1.

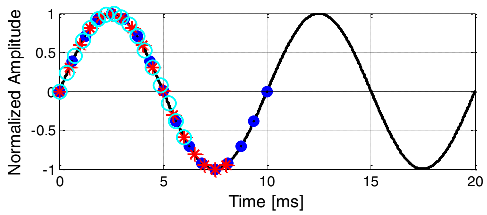

Figure 1. Simulation scheme for obtaining the variation coefficient from a single vibrating scatterer with different values of PRF that cover percentages of the vibrating sinusoid. For all simulations it is assumed that the next data acquisition occurs after each PRP. PRF values of 600 Hz, 700 Hz and 800 Hz are represented by cyan circles, red asterisks and blue dotted points, respectively.

C. *Ensemble length selection*

To study the optimal selection of the ensemble for a given PRF and f_v, the following simulation is proposed: the RF response of a single scatterer to an ultrasound pulse (5MHz) is simulated in MATLAB (8.1.0.604 R2013a, Mathworks, MA, USA). Ensemble lengths commonly available in ultrasound (US) scanners were tested (8, 10, 12, 14 and 16). Finally, the result of the Kasai's variance estimator was evaluated for the following combinations of f_v and PRF: 100 Hz and 600 Hz, 200 Hz and 600 Hz, and 300 and 1 KHz, respectively. The simulation is repeated varying the initial phase of the analyzed signal from 0 to 2π for each f_v.

D. *Sonoelastography: Experiments with a homogeneous vibration field*

The following experiment was designed to avoid any artifacts introduced by an inhomogeneous vibration field in the phantom. Instead of exciting the tissue, the ultrasound transducer is sinusoidally vibrated to simulate a homogeneous vibration field. Sonoelastography imaging experiments were conducted for vibration frequencies of 100, 200, and 300 Hz. PRF values were selected as the most similar frequencies that minimize the variation coefficient as depicted in previous simulations.

The experimental setup is shown in Figure 2-A. A signal generator (B&K Precision 4040B) and amplifier (TEAC A-X500) are connected to a shaker (Brüel & Kjaer 4810) attached to a transducer which scans a homogeneous phantom submerged in unionized water. A point in the middle of the image is randomly selected to observe its spectral variance behavior over time.

For these experiments, two scanners were used in Doppler scanning mode: LOGIQ 9 GE Ultrasound System (GE Healthcare) and Ultrasonix Sonixtouch (Analogic Ultrasound). A homogeneous gelatin phantom was prepared with the following recipe: H_20 1200 mL, Gelatin 514.2 g, NaCl 10.8 g, Cornstarch 24 g [6].

E. *Sonoelastography: Experiments*

Standard sonoelastography imaging experiments were performed using the same instruments as described previously but attaching the shaker to one side of the phantom.

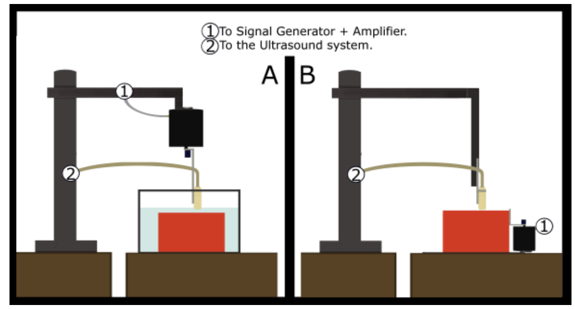

Figure 2. Experimental setup of sonoelastography experiments. **A**: Sonoelastography experiments for a homogeneous vibration field. The homogeneous phantom is in indirect contact with the transducer. The shaker, connected to the signal generator, produces a periodic movement in the transducer. **B**: Sonoelastography experiments. The shaker produces a periodic movement in the phantom. The transducer does not move and scans the vibrating scatterers.

Additionally, the same scanning parameters and phantom were used. In this case, the transducer is detecting the displacements of the vibrating scatterers inside the phantom. Figure 2 B shows the scheme of experimental procedure and Figure 7 shows the sonoelastography frames obtained.

III. Results

A. *Simulation results for the analysis between PRF and f_v*

Figure 3 shows the results depicting the relationship obtained between the PRF and f_v. As observed, the particular points where the variability is minimized are multiples of f_v. For these points, the PRF rate allows the sampling of periodic waveforms in a period of f_v or multiples of it. For these particular combinations of PRF and f_v, the sampling points of the signal are repeated constantly for several acquisitions in time. Therefore, this particular selection of PRF-f_v reduces variability in the sonoelastography results. However, this behavior depends not only on the relationship between PRF and f_v, but also on the number of points sampled for the Kasai's algorithm computation which is defined by the ensemble length.

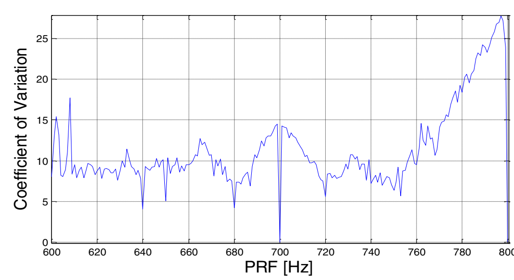

Figure 3. Coefficient of variation as a function of PRF. Simulations are shown for a vibration frequency of 100Hz and ensemble length of 16.

B. *Selection of ensemble length*

Figure 4 shows the variance of Kasai's estimator for shifts in the initial phase of f_v. The variability with time is minimized for ensemble length 8 and 14. In particular, for these two ensemble length values, the sampling packet is a multiple of the vibration frequency, after taking into consideration that two points per cycle are lost, as the data is processed through a two point wall filter and through the autocorrelation algorithm for Kasai variance estimation.

These simulations are repeated for other vibration frequencies and the same behavior is observed. For 200 Hz with PRF = 600 Hz, the optimal ensemble lengths are 8 and 14; for 300 Hz with PRF = 1 KHz, the optimal ensemble length is 12.

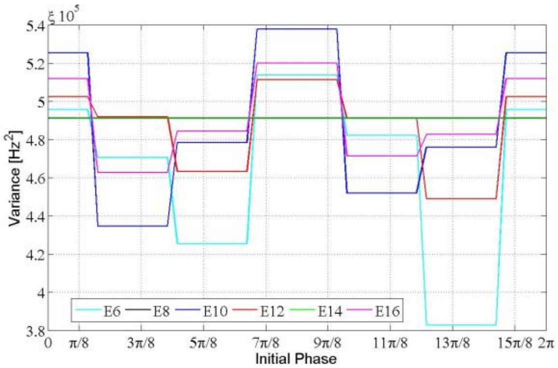

Figure 4. Sonoelastographic variance is presented as a function of the initial phase of the vibration frequency. Simulations developed for a vibration frequency of 100Hz, PRF of 600 Hz and ensemble lengths between 6 and 16.

C. Sonoelastographic results with homogeneous vibration field

Preliminary sonoelastography experiments simulating a homogeneous vibration field were performed with two scanners using the same configuration and varying the ensemble length. Results with f_v = 100 Hz and PRF = 600 Hz are depicted in Figure 5. A similar behavior to the simulation in Figure 4 is verified. Ensemble lengths of 8 and 14 reduce the variability of the sonelastographic values.

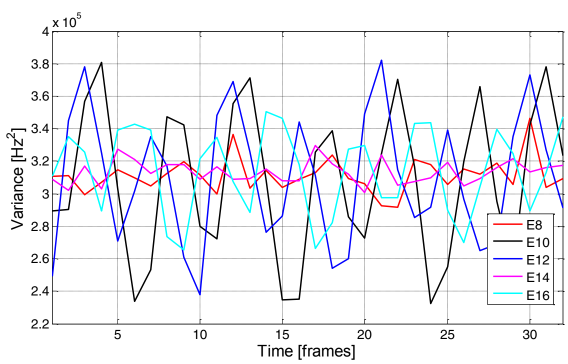

Figure 5. Experimental sonoelastographic results with homogeneous vibration field for a fixed x,y through time due to ensemble length variation with LOGIQ 9 GE Scanner. Configuration: f_v = 100 Hz, PRF = 600 Hz.

Additionally, results for other combinations of PRF, ensemble length and f_v are presented in Table I, minimum variabilities are highlighted in red. Variability is minimized for the case of f_v = 200 Hz and PRF = 600 Hz with ensemble lengths of 8 and 14, and for the case of f_v = 300 Hz and PRF = 1 KHz with ensemble length of 12. These results are similar to the ones from the simulation.

TABLE I. COEFFICIENT OF VARIATION FOR DIFERENT ENSEMBLE LENGTHS.

Scanner	Vibration Frequency	PRF	Ensemble	Coefficient of Variation (%)
Logiq 9 GE	200	600	8	1.2491
			10	16.2629
			12	20.0303
			14	1.5832
			16	11.9243
	300	750	8	24.5821
			10	6.4219
			12	1.0492
			14	8.5931
			16	21.7298
Ultrasonix Sonixtouch	200	600	8	5.9372
			10	31.8290
			12	28.0825
			14	4.8276
			16	30.7911
	300	1000	8	27.6528
			10	30.6849
			12	5.1023
			14	35.4927
			16	29.5412

B. Experimental sonoelastographic results

To describe the impact of these temporal artifacts, qualitative sonoelastography experiments were performed using the LOGIQ 9 scanner. In Figure 6, the variance results for a given sonoelastography point in the middle of the image through time is shown for an f_v of 100 Hz and PRF of 600 Hz. This variance is perceived in all frames, and it is minimized for ensemble length 14, as expected from previous simulations and experiments. Consecutive sonoelastographic images from a cine loop are compared in Figure 7 for ensemble lengths of 14 and 16. The images show the presence of artifacts for ensemble length of 16. However, at ensemble length of 14, the image seems homogeneous in time.

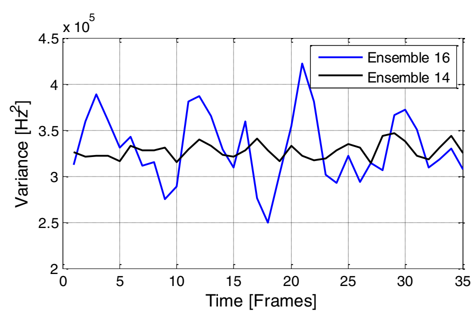

Figure 6. Comparison of sonoelastographic results between ensemble 14 and 16 for all frames. Logiq 9 GE scanner configuration of f_v = 100 Hz, PRF = 600 Hz, ensemble length 14 and ensemble length 16.

This variation performance was quantified through the homogeneity of the sonoelastography images, the results are presented in Table II.

IV. DISCUSSION

The arbitrary selections of PRF and ensemble length parameters can generate temporal artifacts which degrade the quality of sonoelastographic images. Due to the Kasai algorithm's dependence on the initial phase variation for each packet obtained, PRF values should be chosen to match the sampling periodicity required for a given vibration frequency.

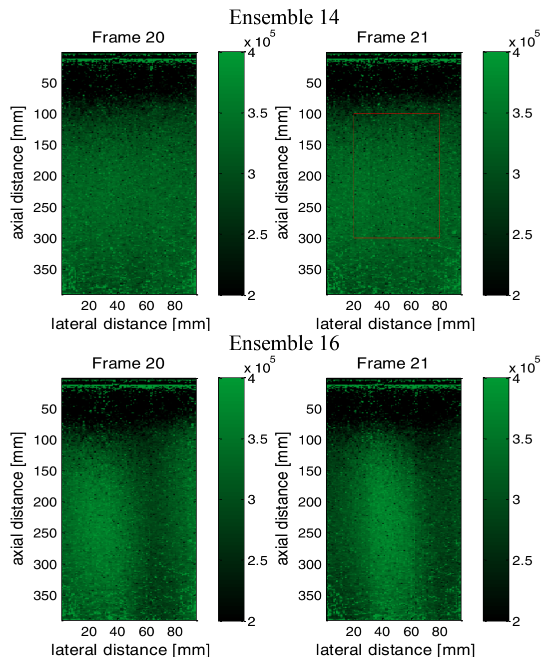

Figure 7. Comparison of sonoelastographic results (expressed in Hz^2) between ensemble lengths of 14 and 16 for two frames of a homogeneous phantom using a Logiq 9 GE setup with f_v of 100 Hz and PRF of 600 Hz. Red box indicates the test region for Table II.

TABLE II. COEFFICIENT OF VARIATION FOR DIFFERENT ENSEMBLE LENGTHS

Scanner	Ensemble length	Variation Coefficient (%)
Logiq 9 GE	8	4.6153
	10	24.2079
	12	22.3897
	14	4.1645
	16	18.3706
Ultrasonix Sonixtouch	8	7.3897
	10	40.0021
	12	42.6415
	14	7.6744
	16	35.2475

Configuration: fv = 100 Hz, PRF = 600 Hz.

Additionally, we propose a rule of thumb to select the ensemble length given a PRF and f_v. With the possible ensemble length options in most scanners varying between 8 and 16, an optimized ensemble length (E) fulfills the empirical relationship,

$$E = n\frac{PRF}{fv} + 2 \qquad [2]$$

where n represents a positive integer. The extra factor of 2 additional points is required to compensate for the loss of end points when a 2 point wall filter is applied to the samples within the packet and the autocorrelation algorithm which is part of the Kasai's estimator. The net result is an integer number of samples per cycle of the vibration.

Furthermore, ensemble lengths defined by the division of PRF by f_v theoretically should minimize temporal artifacts. However, the actual scan sequence in US scanners generates lines of data in a complex pattern with varying time delays between packets. This results in a variation of the initial phase of subsequent packets. Therefore, this relationship without the factor of 2 does generate temporal artifacts in the sonoelastographic images.

The proposed rule of thumb can be readily used with available commercial scanners. Additionally, if the acquisition parameters can be configured, the PRF value could be chosen precisely for each ensemble length and f_v. Therefore, it would be possible to minimize the artifacts due to the Kasai's variance estimator.

In experiments with homogeneous phantoms, the impact of the artifacts is relevant. As seen in Table II and Figure 7, the coefficient of variation may increase up to 42%. These artifacts may also impact on quantitative sonoelastography (Crawling Waves), especially when the Kasai's estimator is used for computing the shear velocity of tissue [9].

V. CONCLUSION

The present study demonstrates that the quality of sonoelastographic images can be heavily affected by an arbitrary selection of scanning parameters (PRF, ensemble length and f_v). The artifacts generated can increase the variability of a homogeneous region from 4% to 42%. An empirical rule is proposed to select these parameters in order to minimize this variability.

REFERENCES

[1] B. Castaneda, K. Hoyt, K. Westesson, L. An, J. Yao, L. Baxter, J. Joseph, J. Strang, D. Rubens, K. J. Parker, "Performance of three-dimensional sonoelastography in prostate cancer detection: a comparison between ex vivo and in vivo experiments," in *Proceedings of the IEEE Ultrasonics Symposium*, pp. 519-522, 2009.

[2] R. M. Lerner, K. J. Parker, J. Holen, R. Gramiak, R. C. Waag, "Sonoelasticity: Medical elasticity images derived from ultrasound signals in mechanically vibrated targets," in *Proceedings of the International Symposium of Acoustical Imaging*, no. 16, pp. 317-327, 1988.

[3] R. Muthupillai, D. J. Lomas, P. J. Rossman, G. J. F., A. Manduca, R. L. Ehman, "Magnetic resonance elastography by direct visualization of propagating acoustic strain waves," *Science*, no. 269, pp. 1854-1857, 1995.

[4] J. M. Schmitt, "OCT elastography: imaging microscopic deformation and strain of tissue," *Optics Express*, no. 6, pp. 199-211, 1998.

[5] A. Partin, Z. Hah, C. T. Barry, D. J. Rubens y K. J. Parker, "Elasticity estimates from images of crawling waves generated by miniature surface sources," *Ultrasound in Medicine & Biology*, no. 40, pp. 685-694, 2014.

[6] J. Ormachea, R. Rojas, P. Rodriguez, R. Lavarello, K. Parker, B. Castaneda, "Shear wave speed estimation from crawling wave Sonoelastography: A comparison between AM-FM dominant component analysis and phase derivation methods," in *Proceedings of the IEEE Ultrasonics Symposium*, pp. 2327 - 2330, 2014.

[7] S. Huang, R. Lerner, K. Parker, "Time domain Doppler estimators of the amplitude of vibrating targets," *Journal of the Acoustical Society of America*, no. 91, pp. 965-974, 1992.

[8] A. C. Chan, E. Y. Lam, V. J. Srinivasan, "Comparison of Kasai autocorrelation and maximum likelihood estimators for Doppler optical coherence tomography," *IEEE Transactions on Medical Imaging*, no. 6, pp. 1033-1042, 2013.

[9] B. Castaneda, L. An, S. Wu, L.L. Baxter, J.L. Yao, J. V. Joseph, K. Hoyt, J. Strang, D. J Rubens, Kevin J Parker, "Prostate cancer detection using crawling wave sonoelastography," in *Proceedings of the SPIE Medical Imaging*, no. 7265, pp. 1301-1310, 2009.